IEEE Access
Multidisciplinary | Rapid Review | Open Access Journal

Received April 10, 2019, accepted June 10, 2019, date of publication June 14, 2019, date of current version July 2, 2019.

Digital Object Identifier 10.1109/ACCESS.2019.2923084

DeepMorse: A Deep Convolutional Learning Method for Blind Morse Signal Detection in Wideband Wireless Spectrum

YE YUAN, ZHONGHUA SUN, ZHIHAO WEI, AND KEBIN JIA, (Member, IEEE)
College of Information and Communication Engineering, Beijing University of Technology, Beijing 100124, China
Beijing Key Laboratory of Computational Intelligence and Intelligent System, Beijing University of Technology, Beijing 100124, China

Corresponding author: Kebin Jia (kebinj@bjut.edu.cn)

This work was supported in part by the National Science Foundation of China under Grant 81871394 and Grant 61672064, and in part by the Beijing Laboratory of Advanced Information Networks under Grant 040000546618017.

ABSTRACT With the recent advances in wireless technologies, high frequency radio has become the primary medium for long-distance communication. Among various types of modulation in signal transmission, morse code stands out due to its simplicity and efficiency in information transmission while costing small bandwidth. In practice, however, it is extremely laborious to locate morse signals in wideband communication. It's a needle in a haystack, if morse code is sent in random carrier waves at random period. To avoid this, automatic morse signal detection has become a challenging task in wireless morse communications, and new solutions could be derived from the latest machine learning techniques. In this paper, we propose a deep learning framework, namely DeepMorse, to blindly detect morse signals in wideband spectrum data. In particular, we first develop a multi-signal sensing module to retrieve signal candidates from wideband spectrum without prior knowledge. Then, we construct a CNN-based module to extract informative features from the located candidates, in order to distinguish the morse signal from other types of modulation. To evaluate the proposed DeepMorse model, we set up a testbed utilizing commercialized long-distance wireless communication devices. The experimental results demonstrate that DeepMorse is able to effectively detect morse signals and outperform the state-of-the-art methods on four real-world datasets.

INDEX TERMS Deep learning, blind signal detection, morse code, wideband wireless spectrum.

I. INTRODUCTION

The recent advancement in wireless technologies has made it possible for long-distance communication using low-cost transceivers. In particular, high frequency radios are capable of broadcasting over large areas through skywave propagation [1], and hence have become the primary medium for a wide range of real-world applications, such as international and regional broadcasting, aviation and marine communication, military radio system, and emergency communication [2], [3]. Among different applications, morse code transmission is one of the most commonly used modulation types to incorporate information in shortwave signals. By encoding information into dashes and dots, morse codes could be efficiently transmitted in a small bandwidth without using special equipment. In order to detect morse signals, traditional approaches focus on manual analysis of the information provided by a spectrum analyzer [4], [5]. Specifically, through wideband spectrum inspection, the time-frequency patterns of such narrowband morse signals can be visualized, recognized, and monitored by expert. In practice, morse signals are usually used in encrypted communications, where no prior information of the initial communication or the bandwidth of the carrier wave is available. It would depend much on the sophisticated professionals to recognize morse codes [6]–[8]. It remains a challenging task for researchers to automatically detect morse signals from wideband spectrum data.

To develop an automatic morse signal detector for wideband radio systems, several challenges should be addressed. First, the frequency information of each carrier signal is unknown, which makes it difficult to distinguish signals based on spectrum. On one hand, the bandwidth of morse signal is narrow and its position is usually stochastically distributed. On the other hand, various irrelevant signals,

The associate editor coordinating the review of this manuscript and approving it for publication was Xiaofei Wang.

in the form of different modulation types, are usually transmitted in different frequency bands simultaneously. Intuitively, an ideal morse detection approach should be able to locate source signals from wideband spectrum and capture representative patterns of each signal to distinguish among the types of modulation. Moreover, the noise in communication environment is often unstable and may vary significantly across temporal and frequency domains, rendering it a challenge to develop a robust detector.

To address the aforementioned challenges, we propose to construct a deep learning model, which has been proved to be effective in modern wireless communications [9]. In particular, convolutional neural networks (CNN) and recurrent neural networks (RNN), have great abilities to extract high-level representative features from noisy and massive data. In this paper, a deep convolutional learning framework, namely DeepMorse, is proposed to blindly detect morse signals from wideband wireless spectrum data. While modulated signals may overlap in time domain, they would show various shape and distribution in spectrum domain. In addition, CNN cannot be directly used for wideband spectrum, since the whole wideband spectrum contains multiple unlocated signals. To this end, the idea is to mimic the practical visual inspection that pays attention to locate source signals at different frequency bands followed by checking each candidate. To the best of our knowledge, this is the first work using deep learning towards blind morse signal detection in wideband spectrum. Specifically, we develop a multi-signal sensing module to retrieve signal candidates with their frequency information from wideband spectrum. We also construct a CNN-based module to extract informative features from the located candidates and incorporate the spatial locality into our framework. Taking advantages of deep learning, the proposed DeepMorse is able to capture morse signals from wideband spectrum, meanwhile distinguish them from other types of modulation.

In order to evaluate the proposed DeepMorse framework, we conduct extensive real-world experiments. In particular, we deploy a long-distance wireless communication infrastructure where several transmitters continuously emit signals to HF wideband, while a wideband receiver collect data from real-world wireless communication environment. The parameters of transmitted signals are not provided to the receiver. The collected spectrum data, after being preprocessed, are fed to our proposed DeepMorse model. Experimental results demonstrate that DeepMorse outperforms the state-of-the-art algorithms, which justify that our proposed framework using deep learning techniques can achieve the level of human experts in blindly detecting morse signals from wideband spectrum.

To sum up, DeepMorse has the following advantages.

- We propose DeepMorse, a convolutional deep learning framework, to mimic the practical blind spectrum visual inspection. To the best of our knowledge, this is the first work using deep learning towards blind morse signal detection in wideband spectrum.
- DeepMorse can not only retrieve morse signals from wideband spectrum without prior knowledge, but also characterize and distinguish morse codes from other types of modulation.
- We set up a testbed using COTS (i.e., commercial off-the-shell) equipment, and collect real-world data. We empirically show that the proposed DeepMorse can effectively detect morse signals and outperform the state-of-the-art methods on four collected datasets.

The rest of the paper is organized as follows: We first review the related work in the next section. In Section II, we describe the system overview of DeepMorse, and present the detail of our proposed methodology in Section IV. The experimental results are then discussed in Section V. Finally, we conclude this work in Section VI.

II. RELATED WORK

In this section, we summarize the literatures related to four research topics: automatic modulation classification, deep learning for spectrum, blind spectrum sensing, and morse signal detection, respectively. We briefly discuss them in the followings.

A. AUTOMATIC MODULATION CLASSIFICATION

Automatic modulation classification (AMC) is one of the core research topics in the area of wireless communication. In general, AMC belongs to a classification problem that aims at automatically identifying the modulation type of transmitted signal. The existing studies of this topic are diverse due to the wide range of civilian and military applications. Traditionally, in order to build the AMC system, researchers use several handcrafted features to train a classifier in a multi-stage fashion. On one hand, different kinds of features are utilized for modulation classification, such as statistical features [10], high-order cumulants [11], [12] and wavelet cyclic features [13]. On the other hand, some well-known classifiers are employed in the AMC system, including support vector machine (SVM) [14], neural networks (NN) [15], k-nearest neighbors (KNN) [16], and decision tree [17]. With any strategy adopted, the design of these methods typically rely on handcrafted feature engineering which is determined based on the specific case and professional domain knowledge.

More recently, significant efforts have been made to explore automatic signal representation techniques using deep learning methods. Such deep features have proven to be more robust than the handcrafted features due to better classification performance. Ali *et al.* [18] adopt stacked autoencoders that combine the in-phase with quadrature constellation points to classify signals received in AWGN and flat-fading channels. Some variants of CNN are employed to analyze signal modulations. Schmidt *et al.* [19] and Akeret *et al.* [20] propose to utilize CNN for the tasks of interference identification in unlicensed bands and radio astronomy, respectively. CNN are also employed to detect characteristic patterns in complex-valued temporal

radio signals proposed by O'Shea *et al.* [21]. Moreover, Rajendran *et al.* [22] and Zhang *et al.* [23] build CNN-based AMC system for low-cost sensors and unmanned aerial vehicles, respectively. Different from the above work, we develop a systematic AMC framework to explore the characteristics of morse codes and distinguish them from other common modulation types. Furthermore, the features learned by the aforementioned deep learning models are directly extracted from narrowband signals where the prior frequency information is given. In contrast, we propose to retrieve unknown morse codes from wideband signals by explicitly utilizing the spatial features learned by convolution operators.

B. DEEP LEARNING FOR SPECTRUM REPRESENTATION

Learning deep representations of spectrum data has gained great attention in many scientific disciplines, since it provides sufficient information carried by frequency contents of signals. Kulin at al. [24] present a deep learning framework for wireless signal identification using spectrum data. The authors discuss the details of spectrum data representation, referred to as the input of deep learning model. To assess the applicability of CNN in the radar emitter classification, Selim at al. [25] propose a spectrum monitoring framework for the detection of radar signals in spectrum sharing scenarios. Regarding to other signal applications, a CNN-based deep learning model is proposed in [26] for human activity recognition using on-node sensor spectrogram. Yuan *et al.* [27] propose multi-view stacked autoencoders to unsupervisedly learn seizure representations from multi-channel EEG spectrum. Different from the existing studies, the data structure of our spectrum data is more complicated, since it consists of multiple source signals. It means that the aforementioned methods cannot be directly used since they make a binary decision for the whole spectrum and hence cannot identify individual signals lied within the wideband spectrum. Compared to the conventional networks, our proposed DeepMorse framework incorporates a multi-signal sensing module to retrieve signal candidates from the given spectrum.

C. BLIND SPECTRUM SENSING

Blind spectrum sensing is one of the most critical components in cognitive radio (CR) that aims at increasing the efficiency of frequency spectrum utilization [28]. It has been widely studied for many years, though there are still many challenges to deal with [29], [30]. Several sensing solutions have been proposed to determine the presence of signals, such as matched filtering [31], cyclostationarity-based detection [32], and energy detection [33]. Among them, energy detection stands out due to its effectiveness in wideband sensing when the information of primary user signals is not provided. Towards this end, different variants of energy-based method are proposed for blind spectrum sensing [34]–[36], and applied in different communication systems including OFDM [37] and massive MIMO [38]. In this work, we propose a new energy-based multi-signal blind sensing algorithm for the task of morse detection, which can be easily integrated into the deep learning module.

D. MORSE SIGNAL DETECTION

Previous research efforts in wireless communications related to morse signal detection are dominantly based on signal processing tools, such as Phase-locked loop, stochastic resonance filters, and time-frequency analysis [39]–[41]. Motivated by recent advances and the remarkable success of machine learning, some handcrafted features are developed to model morse signals in a supervised fashion. In particular, Wei *et al.* [42] present a machine learning method for automatic morse signal detection, and achieve the state-of-the-art performance. The authors propose to train an SVM classifier, named HSVM, using graphical features extracted from morse spectrum, including symmetry features, intermittent features, and distribution features. However, to the best of our knowledge, there have been few deep learning work on blind morse signal detection in wideband spectrum.

III. SYSTEM OVERVIEW

DeepMorse is a wideband blind signal detection system which takes advantage of the superior representation capability of deep learning techniques. The proposed DeepMorse system takes the wideband wireless spectrum data as the input, and outputs inferred narrowband morse signals with their frequency information. Fig. 1 provides an overview of the DeepMorse system. As can be seen, DeepMorse consists of three major components: data collection, data preprocessing, and morse signal detection.

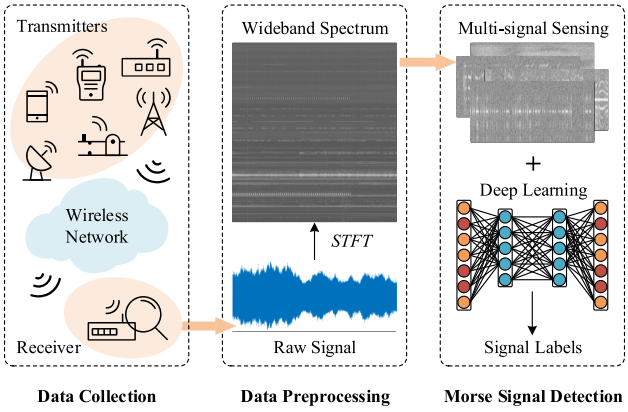

FIGURE 1. Overview of the proposed DeepMorse system. DeepMorse consists of three major components: data collection, data preprocessing, and morse signal detection.

A. DATA COLLECTION

In this paper, we consider a real-world scenario where several heterogeneous transmitters are continuously emitting wireless signals to HF wideband and each of them may generate different types of signal on different center frequencies, e.g., AM, FM, Morse, and Voice. Our DeepMorse system first collects the wideband raw signals from real-world

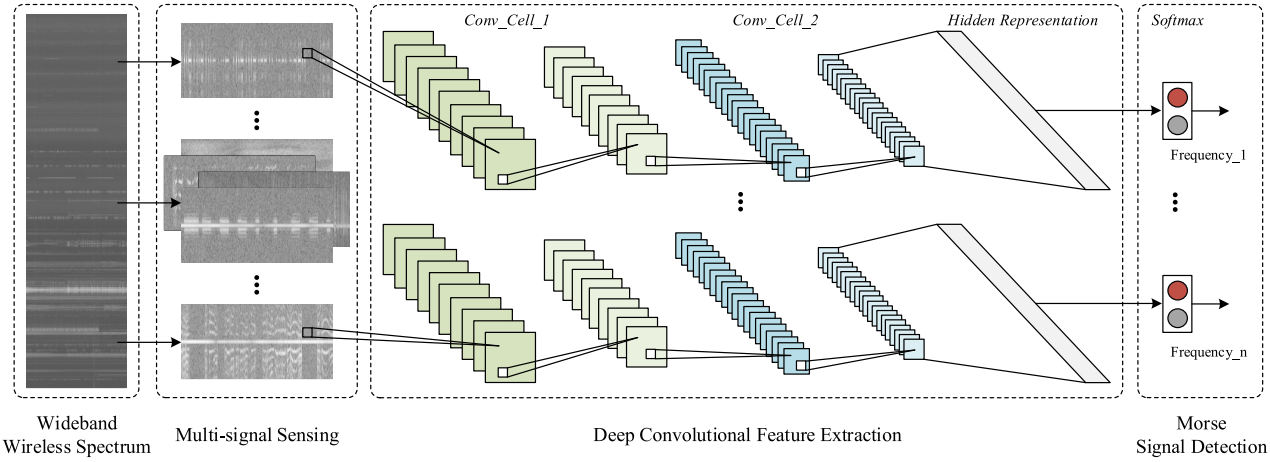

FIGURE 2. Architecture of the proposed DeepMorse model. DeepMorse is a deep learning framework for blind morse signal detection with wideband wireless spectrum data inputs.

communication environment using an off-the-shell receiver and forward them to the data preprocessing component. In our prototype DeepMorse system, we also deploy some morse transmitters to broadcast morse signals in some specific frequency bands (narrow bands). Note that the parameters of those emitted morse signals are not provided for the receiver. Moreover, in usual communication environment, multiple irrelevant signals are usually transmitted in different frequency bands at the same time, which makes the communication channel with variant types of signals. Our goal is to develop a deep learning-based model to blindly retrieve morse codes from those unlabeled and unlocated narrowband signals.

B. DATA PREPROCESSING

Since DeepMorse is designed to detect morse signal in real-time, we first segment the raw signal into fix-length slot utilizing an l-length non-overlapping time window. Then, we utilize short-time Fourier transform (STFT) [43] on each signal segment with n_{fft}-point fast Fourier transform algorithm (FFT). After preprocessing the input data, we obtain a real-valued spectrum $\boldsymbol{S} \in \mathbb{R}^{n_f \times n_t}$ by squaring the magnitude of the complex-valued STFT. It is worth noting that the dimension of $\boldsymbol{S}$ relies on the settings of both the two predefined hyper-parameters: l and n_{fft}. On one hand, increasing the window length l may improve detection performance while would cause delay in real-time applications. On the other hand, the number of FFT points n_{fft} relates to how the signal is represented with different time-frequency resolutions. We discuss the sensitivity of hyper-parameter settings in Section V-F.

C. MORSE SIGNAL DETECTION

In wireless communication, the frequency range of modulations is indefinite. Moreover, background noise usually decays the communication channels and make the spectrum image hard to identify the source signals. This also makes it difficult for traditional machine learning algorithms to characterize the underlying patterns of source signals. To address this challenge, we make use of deep learning techniques to derive discriminative representations from the preprocessed spectrum data. In particular, we propose a deep convolutional learning model, which incorporates a multi-signal sensing algorithm, to automatically locate morse signals from wideband spectrum data. The details of the proposed DeepMorse model are described in Section IV. Given the wideband spectrum data, our model can improve the detection performance by learning informative representations of morse signal.

IV. METHODOLOGY

In this section, we introduce DeepMorse, a deep learning framework for blind morse signal detection with wideband wireless spectrum data inputs. The architecture of the proposed model is illustrated in Fig. 2. In the following subsections, we give the main components of our proposed DeepMorse model.

A. MULTI-SIGNAL SENSING

In practice, the wideband wireless spectrum data usually involves different types of modulation with no prior information to estimate the distribution coefficient of the signal frequency. Under such conditions, there is no efficient way to construct conventional filter banks for signal selection, and directly adopt deep learning methods for signal feature extraction as well. It would be very time-consuming to explicitly monitor all the signal fragments of every center frequency in wideband spectrum, since the computational complexity may grow substantially with the increase in the number of frequency points. Therefore, in order to retrieve multiple signal without estimating the signal components, we develop an energy-based multi-signal sensing module in the proposed DeepMorse model.

In the spectrum image, as we can see in Fig. 2, signal with high signal-noise ratio (SNR) usually corresponds to

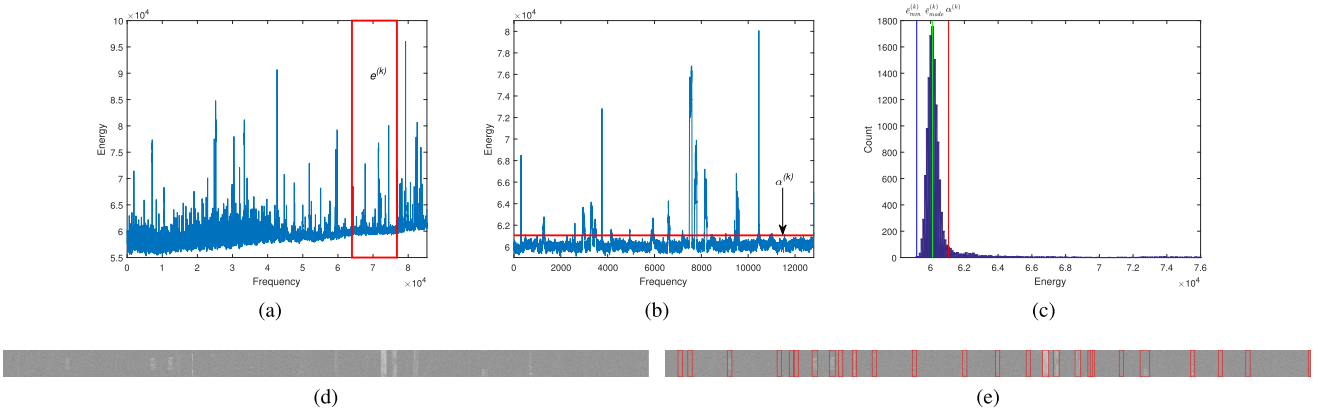

FIGURE 3. Schematic illustrations of the multi-signal sensing procedure in our proposed Deepmorse model. (a) and (b) present the energy vectors of the wideband spectrum and one of its sub-vector, (c) indicates the threshold value based on the histogram of sub-vector, (d) and (e) show the effect diagrams of the sub-vector processed by multi-signal sensing.

bright regions, which describes the power of the signals. In our model, we propose to aware source signals according to the frequency-wise energy distribution in spectrum domain. Fig. 3 illustrates an example of our proposed multi-signal sensing procedure. Given a wideband spectrum $\boldsymbol{S}$, we can obtain its frequency-wise energy vector $\boldsymbol{e} \in \mathbb{R}^{n_f}$ as follows:

$$\boldsymbol{e}_i = \sum_{j=1}^{n_t} \boldsymbol{S}_{i,j}, \tag{1}$$

where $\boldsymbol{S}_{i,j}$ and $\boldsymbol{e}_i$ denote the element of matrix $\boldsymbol{S}$ and vector $\boldsymbol{e}$, respectively. The resulting energy vector reflects the cumulative energy distribution in frequency domain as shown in Fig. 3a. As we can see, on one hand, signals with high SNR exhibit high energy values in vector $\boldsymbol{e}$. Signals with low SNR may be hidden beneath the background (i.e., noise) which is varied over frequencies. In order to eliminate the influence of the communication channel-wise noise for sensing signals, we divide the energy vector into K sub-vectors, denoted as $\{\boldsymbol{e}^{(1)}, \cdots, \boldsymbol{e}^{(K)}\}$ where $\boldsymbol{e}^{(k)} \in \mathbb{R}^{n_f/K}$. Fig. 3b shows an energy vector of sub-vector as example, where the noise has a period of slow variation (relatively stable), and hence we can estimate an appropriate threshold $\boldsymbol{\alpha}^{(k)}$ to determine the presence of signals.

Subsequently, we propose to utilize the histogram to estimate the adaptive threshold $\boldsymbol{\alpha}^{(k)}$ of sub-vector $\boldsymbol{e}^{(k)}$ shown in Fig. 3c. The histogram displays the distribution of energy values in the sub-vector. The x-axis of the histogram represents the range of energy values grouped into several bins, whereas on the y-axis, is the count of these intensities. According to the ITU radio regulations [44] that most signals should be assigned into different frequency bands to prevent interference, the signals should be allocated sparsely in the background. It means that the calculated energy vector contains more noise than source signal, which can be proved from Fig. 3d. Intuitively, the most frequently occurring energy value (highest peak) in the histogram should be concentrated toward the left (low energy) which is the noise portion. Thus, the threshold $\boldsymbol{\alpha}^{(k)}$ can be estimated as follows:

$$\boldsymbol{\alpha}^{(k)} = \bar{\boldsymbol{e}}^{(k)}_{mode} + \lambda(\bar{\boldsymbol{e}}^{(k)}_{mode} - \bar{\boldsymbol{e}}^{(k)}_{min}), \tag{2}$$

where $\bar{\boldsymbol{e}}^{(k)}_{mode}$ and $\bar{\boldsymbol{e}}^{(k)}_{min}$ denote the modal (i.e., max count) and minimum center bins (i.e., energy values) of histogram. Here in Eq. (2), λ is the hyper-parameter that control the distance between $\boldsymbol{\alpha}^{(k)}$ and $\bar{\boldsymbol{e}}^{(k)}_{mode}$. In addition, we employ the Freedman-Diaconis rule [45] to determine the number of bins b in histogram, since it is more suitable for data with long-tailed distributions.

Based on the estimated threshold $\boldsymbol{\alpha}^{(k)}$, we can retrieve a set of source signal fragments $\boldsymbol{X}^{(k)}$ with their frequency information $\boldsymbol{I}^{(k)}$ from each sub-vector $\boldsymbol{S}^{(k)}$, as shown in Fig. 3e. Moreover, in order to unify the dimensions of fragments as input for the following CNN module, we limit the bandwidth ω to 2KHz. In particular, we expand the captured fragments on frequency center if their bandwidths are less than ω, otherwise we resize the larger fragments using bilinear interpolation [46]. The detailed steps of the proposed multi-signal sensing module is summarized in algorithm 1. In this way, a set of narrowband signal fragments $\boldsymbol{X} = \{\boldsymbol{x}_1, \cdots, \boldsymbol{x}_F\}$ where $\boldsymbol{x}_f \in \mathbb{R}^{n_\omega \times n_t}$ is retrieved from wideband spectrum. All the captured fragments are treated as morse signal candidates, which enable the following CNN module to further identify morse signals. Compared to the whole wideband spectrum, the size of the located candidates is relatively small and it is suitable for the input of CNN.

B. DEEP CONVOLUTIONAL FEATURE EXTRACTION

In order to extract local spatial features from spectrum, we present a CNN-based module to extract convolutional features from the retrieved spectrum fragments. We construct the CNN encoders by stacking a series of convolutional-nonlinear-pooling cells with different filter maps. Specifically, a 2-cell CNN architecture is adopted to extract latent features from the located candidates. Unlike nature images that usually involve complicated and abstract geometrical

Algorithm 1 Multi-Signal Sensing

Input: wideband wireless spectrum $\boldsymbol{S}$ with dimension (n_f, n_t), number of sub-vector $K = 7$, bandwidth $\omega = 2$kHz
Output: Signal fragment set $\boldsymbol{X}$, frequency information set $\boldsymbol{I}$

Compute the energy vector $\boldsymbol{e}$ of spectrum $\boldsymbol{S}$ using Eq. (1)
Divide $\boldsymbol{e}$ into K sub-vectors: $\{\boldsymbol{e}^{(1)}, \cdots, \boldsymbol{e}^{(K)}\}$
Initialize: $\boldsymbol{X} \leftarrow \{\}, \boldsymbol{I} \leftarrow \{\}$
for each $\boldsymbol{e}^{(k)} \in \boldsymbol{e}$ **do**
    Initialize: $\boldsymbol{X}^{(k)} \leftarrow \{\}, \boldsymbol{I}^{(k)} \leftarrow \{\}, flag \leftarrow 0$, $(l_{start}, l_{end}) \leftarrow (-1, -1), \boldsymbol{x} \leftarrow []$
    Compute the histogram and threshold $\boldsymbol{\alpha}^{(k)}$ of $\boldsymbol{e}^{(k)}$ using Eq. (2)
    for each $\boldsymbol{e}_i^{(k)} \in \boldsymbol{e}^{(k)}$ **do**
        if $\boldsymbol{e}_i^{(k)} \geq \boldsymbol{\alpha}^{(k)}$ **then**
            if $flag == 0$ **then**
                $l_{start} \leftarrow i, flag \leftarrow 1$
            end if
        else
            if $flag == 1$ **then**
                $l_{end} \leftarrow i, flag \leftarrow 0$
                $\boldsymbol{e}_{l_{center}}^{(k)} \leftarrow \text{argmax}(\boldsymbol{S}^{(k)}[l_{start} : l_{end}, :])$
                if $l_{end} - l_{start} < \omega$ **then**
                    $\boldsymbol{x} \leftarrow \boldsymbol{S}^{(k)}[l_{center} \pm 0.5\omega, :]$
                else

$\boldsymbol{x} \leftarrow \text{Resize}(\boldsymbol{S}^{(k)}[l_{start} : l_{end}, :], [\omega, :])$
                end if
                $\boldsymbol{X}^{(k)} \leftarrow \boldsymbol{X}^{(k)} \cup \boldsymbol{x}$
                $\boldsymbol{I}^{(k)} \leftarrow \boldsymbol{I}^{(k)} \cup ((k-1)n_f/K) + l_{center}$
            end if
        end if
    end for
    $\boldsymbol{X} \leftarrow \boldsymbol{X} \cup \boldsymbol{X}^{(k)}$
    $\boldsymbol{I} \leftarrow \boldsymbol{I} \cup \boldsymbol{I}^{(k)}$
end for

structures, the located spectrum is characterized by local textural features. Although the modulation textures in spectrum are intuitively easy for experts to perceive, formulating a formal definition as handcrafted features is not trivial. This encourages the use of CNN to automatically learn spatial features from spectrum and hence distinguish textures of morse signal from other types of modulation. Since the textures of the candidates are characterized by fine grained low-level features, adopting a 2-cell CNN architecture is enough for our morse signal detection task.

Given a located spectrum fragment $\boldsymbol{x}$, the latent features of the r-th feature map in the first cell, denoted as $\boldsymbol{h}_{c_1}^{(r)}$, can be obtained as follows:

$$\boldsymbol{h}_{c_1}^{(r)} = \text{Pooling}_{c_1}(f(\boldsymbol{x} * \boldsymbol{W}_{c_1}^{(r)} + \boldsymbol{b}_{c_1}^{(r)})), \tag{3}$$

where $*$ is the convolution operator, $f(\cdot)$ denotes the ReLU function (i.e., $f(z) = \max(0, z)$), and $\boldsymbol{W}_{c_1}^{(r)}$ and $\boldsymbol{b}_{c_1}^{(r)}$ are the learnable parameters. Here in Eq. (3), the convolution operator with sets of learnable filter banks are utilized to extract local features from the input spectrum, and the pooling operator (max pooling) is used for down-sampling. Similarity, we can obtain the latent features of the q-th feature map in the second cell $\boldsymbol{h}_{c_2}^{(q)}$ based on all the captured features in the previous cell, as follows:

$$\boldsymbol{h}_{c_2}^{(q)} = \text{Pooling}_{c_2}(f(\sum_{r=1}^{R}(\boldsymbol{h}_{c_1}^{(r)} * \boldsymbol{W}_{c_2}^{(q)}) + \boldsymbol{b}_{c_2}^{(q)})), \tag{4}$$

where R is the total number of feature map in the previous cell, $\boldsymbol{W}_{c_2}^{(q)}$ and $\boldsymbol{b}_{c_2}^{(q)}$ are the learnable weight matrix and bias vector, respectively. Subsequently, all the latent features extracted using Eq. (4) are flattened to derive the hidden representation $\boldsymbol{h}_p \in \mathbb{R}^p$ by:

$$\boldsymbol{h}_p = f(\boldsymbol{W}_p \text{Flatten}(\boldsymbol{h}_{c_2}^{(1:Q)}) + \boldsymbol{b}_p), \tag{5}$$

where Q is the total number of feature maps in the last cell, $\boldsymbol{W}_p$ and $\boldsymbol{b}_p$ are the parameters to be learned. Note that the dimension of $\boldsymbol{h}_{c_2}^{(q)}$ and $\boldsymbol{b}_{c_2}^{(q)}$ relies on the structure configuration of CNN, which is given in Section V-D.

C. LEARNING AND DETECTION

Given the hidden representation $\boldsymbol{h}_p$ calculated by Eq. (5), we feed it through the softmax layer to identify morse signal in the located candidate, as follows:

$$\hat{\boldsymbol{y}} = \text{Softmax}(\boldsymbol{W}_s \boldsymbol{h}_p + \boldsymbol{b}_s), \tag{6}$$

where $\boldsymbol{W}_s \in \mathbb{R}^{|\mathcal{C}| \times p}$ and $\boldsymbol{b}_s \in \mathbb{R}^{|\mathcal{C}|}$ are the parameters to be learned. Here we employ cross-entropy to measure the loss between the ground truth $\boldsymbol{y}$ and the $\hat{\boldsymbol{y}}$ obtained by Eq. (6). Formally, given M training sets $\{\boldsymbol{x}_1^{(m)}, \boldsymbol{x}_2^{(m)}, \cdots, \boldsymbol{x}_{F^{(m)}}^{(m)}\}_{m=1}^{M}$ with their corresponding labels $\{\boldsymbol{y}_1^{(m)}, \boldsymbol{y}_2^{(m)}, \cdots, \boldsymbol{y}_{F^{(m)}}^{(m)}\}_{m=1}^{M}$, the cost function can be represented as:

$$J_{DeepMorse}(\boldsymbol{x}_1^{(1)}, \cdots, \boldsymbol{x}_{F^{(1)}}^{(1)}, \cdots, \boldsymbol{x}_1^{(M)}, \cdots, \boldsymbol{x}_{F^{(M)}}^{(M)})$$
$$= -\frac{1}{M}\sum_{i=1}^{M}\frac{1}{F^{(i)}}\sum_{f=1}^{F^{(i)}}\left[\boldsymbol{y}_f^{\top}\log\hat{\boldsymbol{y}}_f + (\boldsymbol{1} - \boldsymbol{y}_f)^{\top}\log(\boldsymbol{1} - \hat{\boldsymbol{y}}_f)\right]$$

V. EXPERIMENTS AND DISCUSSIONS

In this section, we carry out experiments on four datasets collected by a real-world testbed to demonstrate the efficacy of our DeepMorse framework. We first describe the datasets used in the experiments, then introduce the baselines, evaluation criteria, and implementation details. We finally show the experimental results and discuss the model sensitivity.

A. DATASET DESCRIPTION

In the experiments, four datasets are collected from a real-world testbed to validate our proposed DeepMorse model. The raw signals are received from a COTS 400W shortwave communication platform consisting of several transmitters and one wideband receiver. In order to fully evaluate our model under different real-world environments,

TABLE 1. Statistics of each experimental dataset ($n_{fft} = 128K$, $l = 8.532sec$).

	Datasets			
Description	5M	7M	9M	12M
Frequency center	5 MHz	7 MHz	9 MHz	12 MHz
Frequency width	2 MHz	2 MHz	2 MHz	2 MHz
Sample Rate	2.56 MHz	2.56 MHz	2.56 MHz	2.56 MHz
Time duration	102 sec	102 sec	102 sec	102 sec
# of samples	5,171	8,582	7,277	1,898
- # of morse samples	2,520	4,968	3,192	768
- # of non-morse samples	2,651	3,614	4,085	1,130
- # of raw features	85×400	85×400	85×400	85×400

we collect data with different settings including center frequency, transmission distance, season, and time of day. The collected data are manually labeled to train and test our proposed deep learning model. Moreover, since the morse signals in our scenarios are treated as rare events, we use data augmentation, including the operations of rotations and Gaussian noising, to enlarge the number of morse samples. Finally, we present the statistical information of the collected datasets in Table 1.

B. BASELINES

We compare our proposed DeepMorse model with five commonly used feature learning baselines:

Support Vector Machine (SVM) [47]. SVM is a classic machine learning method. Here we first reshape the input data into a vector space, and use them to train a binary SVM model.

Principal Component Analysis [48] + SVM (PSVM). PCA is a widely adopted mechanism to extract features from high dimensional data. For the sake of fairness, we select top-p related components as features to train the SVM model, namely PSVM.

HSVM [42]. This method is the state-of-the-art morse detection model using handcrafted feature engineering to exclude redundant and irrelevant information from raw data.

Deep Neural Networks (DNN) [49]. DNN is a standard deep learning model that incorporate multiple hidden layers to enhance feature representation. We train a 3-layer DNN model for morse detection. We set the size of each hidden layer as $4p$, $2p$, and p, respectively.

Stacked Autoencoders (SAE) [50]. SAE is a widely used deep learning networks stacked by several basic autoencoder (AE) layers. Similarly, we train a 3-layer SAE model to minimize both the reconstruction and classification errors.

C. EVALUATION CRITERIA

To quantify the performance, four evaluation criteria, including precision, recall, F1-score, and accuracy, are adopted as the evaluation criteria. Moreover, the area-under-the-curve of precision-recall (AUC-PR) and receiver operator characteristic (AUC-ROC) are also utilized to evaluate each approach.

D. IMPLEMENTATION DETAILS

We implement the proposed DeepMorse model using Pytorch [51]. During the training process, Adadelta optimization algorithm [52] with mini-batch (the batch size is 100) is used to optimize the parameters. For all the datasets, we first shuffle all the samples and conduct 5-fold cross validation. We also deploy 0.5 dropout, 0.95 momentum, and 0.001 weight decay to prevent overfitting. The configurations of CNN in DeepMorse is presented in Table 2, and we use $p = 128$ for baselines and our model.

TABLE 2. CNN structure of the proposed DeepMorse model.

Cell No.	Conv	Non-linear	Pooling
1	$5 \times 5 \times 16$	ReLU	2×2
2	$5 \times 5 \times 32$	ReLU	2×2

E. DETECTION PERFORMANCE

We report the comparison results of our proposed DeepMorse model and baselines in Table 3. Here we show the average performance of each method based on 5-fold cross validation. We can observe that DeepMorse achieves the best performance in terms of all the evaluation measurements.

Given the results of baselines, we can see that the plain SVM performs well at the original high-dimensional input data. However, after reducing the dimensionality to the same one as ours through PCA, PSVM performs worse. It means that simply adopting PCA cannot make SVM separate the morse and non-morse labels in the projected feature space. We can also see that the NN-based models (i.e., DNN and SAE) perform much worse than the SVM-based models due to the curse of dimensionality. Compared with DNN, the limited improvement of SAE demonstrates that the layer-wise reconstruction procedure helps deep structure learn relative better feature representations from spectrums. Not surprisingly, HSVM works well on morse detection as also reported in previous work [42], which suggests the effectiveness of handcrafted engineering to extract meaningful features.

From the results, our DeepMorse model outperforms all the baselines. For example, DeepMorse achieves the best accuracy of 0.9718 on the 7M datasets, compared with 0.9539 and 0.8658 obtained by the HSVM and SVM baselines, respectively. Compared the results among all the datasets, DeepMorse achieves a robust performance under different wireless environments. The reason is that the spatial information of signal spectrum is remained by locally-connected neural networks. Fig. 4 and Fig. 5 illustrate the ROC and PR curves on all the datasets, respectively. From the ROC curves shown in Fig. 4, we can observe that the true positive rate increases fast from the start, which means that DeepMorse has great abilities to capture distinctive information from spectrum. Regarding the PR curves shown in Fig. 5, the precision rate of DeepMorse decreases more slowly at the beginning than the others. This again illustrates the effectiveness of our

TABLE 3. Performance comparisons on four real-world datasets.

Method	Dataset	Evaluation Measurements					
		AUC-ROC	AUC-PR	Precision	Recall	F1-score	Accuracy
SVM	5M	0.9801	0.9797	0.9743	0.8679	0.9179	0.9244
	7M	0.9421	0.9617	0.9186	0.8428	0.8791	0.8658
	9M	0.9539	0.9809	0.9280	0.9527	0.9402	0.9095
	12M	0.9735	0.9663	0.9555	0.7645	0.8481	0.8899
PSVM	5M	0.9172	0.9190	0.9135	0.7889	0.8464	0.8606
	7M	0.8114	0.8350	0.8086	0.7178	0.7604	0.7382
	9M	0.8482	0.9418	0.8301	0.9248	0.8746	0.8022
	12M	0.8953	0.8665	0.8502	0.6564	0.7399	0.8146
DNN	5M	0.5219	0.7325	0.2563	0.5000	0.3389	0.5127
	7M	0.4999	0.7893	0.2894	0.5000	0.3666	0.5789
	9M	0.5005	0.8729	0.3732	0.5000	0.4274	0.7463
	12M	0.5052	0.7004	0.2977	0.5000	0.3732	0.5954
SAE	5M	0.8999	0.9086	0.8545	0.7548	0.7935	0.8113
	7M	0.5113	0.6790	0.2894	0.5000	0.3666	0.5789
	9M	0.7276	0.8739	0.3732	0.5000	0.4274	0.7463
	12M	0.7401	0.6521	0.6575	0.5598	0.5666	0.6802
HSVM	5M	0.9902	0.9912	0.9862	0.9591	0.9724	0.9735
	7M	0.9867	0.9897	0.9717	0.9479	0.9597	0.9539
	9M	0.9871	0.9930	0.9807	0.9846	0.9826	0.9740
	12M	0.9916	0.9910	0.9725	0.9584	0.9652	0.9721
DeepMorse	5M	**0.9926**	**0.9931**	**0.9872**	**0.9786**	**0.9828**	**0.9834**
	7M	**0.9893**	**0.9918**	**0.9838**	**0.9672**	**0.9754**	**0.9718**
	9M	**0.9923**	**0.9944**	**0.9876**	**0.9925**	**0.9900**	**0.9850**
	12M	**0.9946**	**0.9945**	**0.9961**	**0.9792**	**0.9875**	**0.9900**

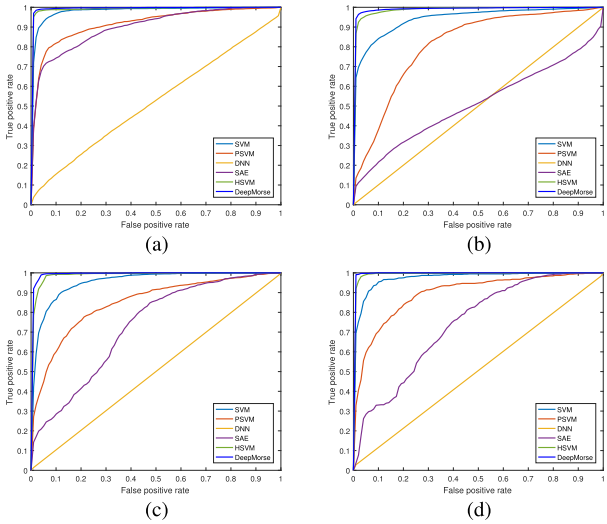

FIGURE 4. ROC curves of the proposed method and the baselines on four datasets. (a) 5M. (b) 7M. (c) 9M. (d) 12M.

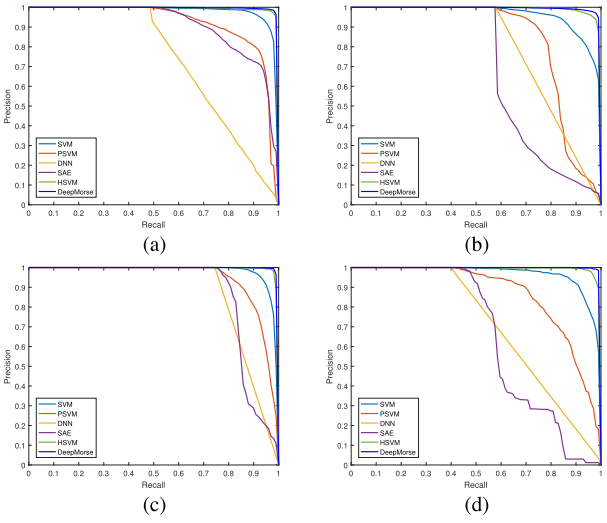

FIGURE 5. PR curves of the proposed method and the baselines on four datasets. (a) 5M. (b) 7M. (c) 9M. (d) 12M.

DeepMorse model. Furthermore, based on Table 3, the proposed DeepMorse method consistently achieves the best AUC in terms of the ROC and PR on different datasets, demonstrating an effective method in the task of morse detection.

F. SENSITIVITY ANALYSIS

In this subsection, we discuss the effects of various hyper-parameter choices in DeepMorse, including the dimensionality of hidden representation p, the length of time

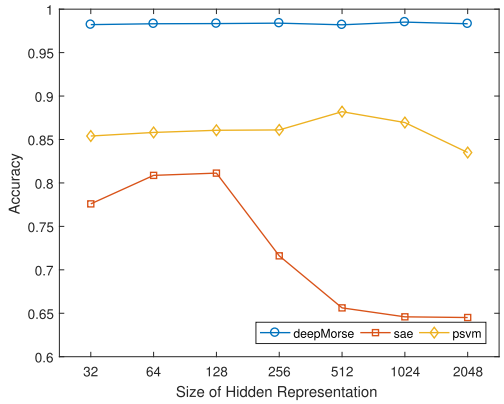

FIGURE 6. Performance variations with different parameter settings on the 5M dataset. (a) Sensitivity analysis with different sizes of hidden layer. (b) Sensitivity analysis with different time window lengths. (c) Sensitivity analysis with different numbers of FFT points.

window l, and the number of FFT points n_{fft}. Specifically, we plot accuracy results of the DeepMorse under different hyper-parameter settings on the 5M dataset, as shown in Fig. 6. We ignore the results of DNN because of the bad performance. The basic configuration is mentioned in Section V-D, and we vary one hyper-parameter while keeping others fixed to the basic configuration.

Hidden representation size p. We report the influence of p in Fig. 6a. From the figure, we can observe that different models get their best accuracy in different sizes of hidden representation. Specifically, PCA achieves the best accuracy when p is 512, and 128 is the optimal choice for SAE. When p is too large, the performance of SAE decreases significantly due to the curse of dimensionality. We can see that our proposed DeepMorse framework is able to achieve comparable results with relative small hidden units, and gets stable performance under different settings of p.

Time window length l. Fig. 6b illustrates the change of accuracy for different values of time window length l. From the figure, we can see that decreasing the time length degrades the performance of all of the algorithms, since the short time leads to insufficient information provided by spectrum to train the models. We can also obverse that different nature of feature extraction strategies contributes to different performance variations under different configurations. In particular, as we decrease the length, both SAE and PSVM lack the capability of capturing representative features, resulting in limited performance on accuracy. Moreover, we find the performance bifurcation point of HSVM when the length is less than 1 second. It means that the handcrafted features extracted by HSVM cannot guarantee consistently good performance across different situations. This can also be found from the performance of SVM using raw features, where the accuracy decreases dramatically when l is getting smaller. In contrast, our proposed DeepMorse model consistently beats the baselines. This results from the fact that CNN has the strong capability of model generalization.

Number of FFT points n_{fft}. Fig. 6c shows the experimental results of n_{fft}. From the figure, we can see the similar trends of all the models under the influence from $32K$ to $128K$. This demonstrates that spectrum with different time and frequency solutions may carry different amount of information describing morse signals. As we increase the number of FFT points from $128K$ to $512K$, all the models shows an increasing modeling power except HSVM. This means that a larger value of n_{fft} leads to worse capture of critical information using HSVM. Moreover, our proposed DeepMorse model still get better performance than the others.

According to the overall sensitivity analysis, we conclude that our proposed DeepMorse model achieves the highest accuracy and DeepMorse's performance is robust to choice of the hyper-parameters in a wide range of values. Comparing to the more volatile performance of HSVM, we can see that DeepMorse not only improves the performance, but also stabilizes it as well.

VI. CONCLUSION

In this paper, we present a deep learning-based framework, namely DeepMorse, to address the challenges of blind detection of morse signals from wideband spectrum data. DeepMorse aims at mimicking the practical blind spectrum visual inspection that pays attention to locate source signals in different frequency bands followed by detailed check of each candidate. With the help of our proposed multi-signal sensing and deep convolutional feature extraction modules,

DeepMorse is able to independently locate morse signals in wideband spectrum without prior knowledge, and capture representative patterns of each signal to distinguish morse codes from other types of modulation. For validation, a real-world testbed is built using commercialized long-distance wireless communication infrastructure, and we collect four datasets with different scenario settings. Experimental results on the four collected datasets demonstrate that DeepMorse can achieve better and more robust performance than the stat-of-the-art morse detection approaches, and hence proves the effectiveness of DeepMorse for blind detection of morse signals.

Regarding the robustness of our framework, we first retrieve signal candidates from wideband spectrum by the multi-signal sensing module, then feed the candidates to the CNN module for feature extraction and signal detection. Since the located candidates belong to narrowband signals, the CNN module in DeepMorse is able to deal with different settings. In our future work, as the proposed DeepMorse framework is task-oriented, it is applicable to other applications with similar blind detection scenario, especially in spectrum sensing where monitoring and understanding the spectrum usage is still a major challenge in cognitive radio.

Regarding the hardware capability in our experiments, we build a real-world testbed using a COTS 400W shortwave communication platform. It means that it is possible and available to implement such wideband sensing scenario in practice, which has been widely used in many real-world applications. For the cases where the equipment cannot capture the whole spectrum of interest, the collected spectrum would be a part of the whole spectrum, and hence the size of the collected spectrum would be relatively small. The proposed multi-signal sensing module is able to retrieve signal candidates from the partial wideband spectrum by reducing the number of sub-vector K. Furthermore, one solution of the equipment issue is that we can adopt the multi-signal sensing module for multiple partial spectrums (collected by multiple receivers) in parallel to obtain signal candidates from the whole spectrum. We will investigate more test related to this issue in our future work.

ACKNOWLEDGMENT

The authors would like to thank the anonymous reviewers, and NVIDIA Corporation for the donation of the Titan Xp GPU.

REFERENCES

[1] J. S. Seybold, *Introduction to RF Propagation*. Hoboken, NJ, USA: Wiley, 2005.
[2] M. Zhao, A. Kumar, T. Ristaniemi, and P. H. J. Chong, "Machine-to-machine communication and research challenges: A survey," *Wireless Pers. Commun.*, vol. 97, no. 3, pp. 3569–3585, Dec. 2017.
[3] G. Baldini, S. Karanasios, D. Allen, and F. Vergari, "Survey of wireless communication technologies for public safety," *IEEE Commun. Surveys Tuts.*, vol. 16, no. 2, pp. 619–641, 2nd Quart., 2014.
[4] A. Goldsmith, *Wireless Communications*. Cambridge, U.K.: Cambridge Univ. Press, 2005.
[5] H. Zhongyu, *Modern Short Wave Communication*. Beijing, China: National Defense Industry Press, 2003.
[6] E. Axell, G. Leus, E. G. Larsson, and H. V. Poor, "Spectrum sensing for cognitive radio: State-of-the-art and recent advances," *IEEE Signal Process. Mag.*, vol. 29, no. 3, pp. 101–116, May 2012.
[7] O. A. Dobre, A. Abdi, Y. Bar-Ness, and W. Su, "Survey of automatic modulation classification techniques: Classical approaches and new trends," *IET Commun.*, vol. 1, no. 2, pp. 137–156, Apr. 2007.
[8] C. Weber, M. Peter, and T. Felhauer, "Automatic modulation classification technique for radio monitoring," *Electron. Lett.*, vol. 51, no. 10, pp. 794–796, 2015.
[9] T. O'Shea and J. Hoydis, "An introduction to deep learning for the physical layer," *IEEE Trans. Cogn. Commun. Netw.*, vol. 3, no. 4, pp. 563–575, Dec. 2017.
[10] J. Lopatka and M. Pedzisz, "Automatic modulation classification using statistical moments and a fuzzy classifier," in *Proc. 5th Int. Conf. Signal Process. (WCCC-ICSP)*, vol. 3, Aug. 2000, pp. 1500–1506.
[11] S. Huang, Y. Yao, Z. Wei, Z. Feng, and P. Zhang, "Automatic modulation classification of overlapped sources using multiple cumulants," *IEEE Trans. Veh. Technol.*, vol. 66, no. 7, pp. 6089–6101, Jul. 2016.
[12] A. Swami and B. M. Sadler, "Hierarchical digital modulation classification using cumulants," *IEEE Trans. Commun.*, vol. 48, no. 3, pp. 416–429, Mar. 2000.
[13] L. Zhou and H. Man, "Wavelet cyclic feature based automatic modulation recognition using nonuniform compressive samples," in *Proc. IEEE 78th Veh. Technol. Conf. (VTC Fall)*, Sep. 2013, pp. 1–6.
[14] C.-S. Park, W. Jang, S.-P. Nah, and D. Y. Kim, "Automatic modulation recognition using support vector machine in software radio applications," in *Proc. 9th Int. Conf. Adv. Commun. Technol.*, vol. 1, Feb. 2007, pp. 9–12.
[15] A. Fehske, J. Gaeddert, and J. H. Reed, "A new approach to signal classification using spectral correlation and neural networks," in *Proc. 1st IEEE Int. Symp. New Frontiers Dyn. Spectr. Access Netw.*, Nov. 2005, pp. 144–150.
[16] S. Kharbech, I. Dayoub, M. Zwingelstein-Colin, and E. P. Simon, "On classifiers for blind feature-based automatic modulation classification over multiple-input–multiple-output channels," *IET Commun.*, vol. 10, no. 7, pp. 790–795, May 2016.
[17] Z. Zhu, M. W. Aslam, and A. K. Nandi, "Genetic algorithm optimized distribution sampling test for M-QAM modulation classification," *Signal Process.*, vol. 94, pp. 264–277, Jan. 2014.
[18] A. Ali, F. Yangyu, and S. Liu, "Automatic modulation classification of digital modulation signals with stacked autoencoders," *Digit. Signal Process.*, vol. 71, pp. 108–116, Dec. 2017.
[19] M. Schmidt, D. Block, and U. Meier, "Wireless interference identification with convolutional neural networks," 2017, *arXiv:1703.00737*. [Online]. Available: https://arxiv.org/abs/1703.00737
[20] J. Akeret, C. Chang, A. Lucchi, and A. Refregier, "Radio frequency interference mitigation using deep convolutional neural networks," *Astron. Comput.*, vol. 18, pp. 35–39, Jan. 2017.
[21] T. J. O'Shea, J. Corgan, and T. C. Clancy, "Convolutional radio modulation recognition networks," in *Proc. Int. Conf. Eng. Appl. Neural Netw.* Cham, Switzerland: Springer, 2016, pp. 213–226.
[22] S. Rajendran, W. Meert, D. Giustiniano, V. Lenders, and S. Pollin, "Distributed deep learning models for wireless signal classification with low-cost spectrum sensors," 2017, *arXiv:1707.08908*. [Online]. Available: https://arxiv.org/abs/1707.08908
[23] D. Zhang, W. Ding, B. Zhang, C. Xie, H. Li, C. Liu, and J. Han, "Automatic modulation classification based on deep learning for unmanned aerial vehicles," *Sensors*, vol. 18, no. 3, p. 924, 2018.
[24] M. Kulin, T. Kazaz, I. Moerman, and E. De Poorter, "End-to-end learning from spectrum data: A deep learning approach for wireless signal identification in spectrum monitoring applications," *IEEE Access*, vol. 6, pp. 18484–18501, 2018.
[25] A. Selim, F. Paisana, J. A. Arokkiam, Y. Zhang, L. Doyle, and L. A. DaSilva, "Spectrum monitoring for radar bands using deep convolutional neural networks," 2017, *arXiv:1705.00462*. [Online]. Available: https://arxiv.org/abs/1705.00462
[26] D. Ravì, C. Wong, B. Lo, and G.-Z. Yang, "A deep learning approach to on-node sensor data analytics for mobile or wearable devices," *IEEE J. Biomed. Health Inform.*, vol. 21, no. 1, pp. 56–64, Jan. 2017.
[27] Y. Yuan, G. Xun, K. Jia, and A. Zhang, "A multi-view deep learning method for epileptic seizure detection using short-time Fourier transform," in *Proc. 8th ACM Int. Conf. Bioinformatics, Comput. Biol., Health Inform.*, 2017, pp. 213–222.
[28] J. Mitola and G. Q. Maguire, Jr., "Cognitive radio: Making software radios more personal," *IEEE Pers. Commun.*, vol. 6, no. 4, pp. 13–18, Apr. 1999.

[29] H. Sun, A. Nallanathan, C.-X. Wang, and Y. Chen, "Wideband spectrum sensing for cognitive radio networks: A survey," *IEEE Wireless Commun.*, vol. 20, no. 2, pp. 74–81, Apr. 2013.

[30] R. Umar and A. U. H. Sheikh, "A comparative study of spectrum awareness techniques for cognitive radio oriented wireless networks," *Phys. Commun.*, vol. 9, pp. 148–170, Dec. 2013.

[31] T. Yucek and H. Arslan, "A survey of spectrum sensing algorithms for cognitive radio applications," *IEEE Commun. Surveys Tuts.*, vol. 11, no. 1, pp. 116–130, 1st Quart., 2009.

[32] Z. Tian, Y. Tafesse, and B. M. Sadler, "Cyclic feature detection with sub-Nyquist sampling for wideband spectrum sensing," *IEEE J. Sel. Topics Signal Process.*, vol. 6, no. 1, pp. 58–69, Feb. 2012.

[33] H. Urkowitz, "Energy detection of unknown deterministic signals," *Proc. IEEE*, vol. 55, no. 4, pp. 523–531, Apr. 1967.

[34] J. Nikonowicz and M. Jessa, "A novel method of blind signal detection using the distribution of the bin values of the power spectrum density and the moving average," *Digit. Signal Process.*, vol. 66, pp. 18–28, Jul. 2017.

[35] Y. Zeng, Y. C. Liang, and R. Zhang, "Blindly combined energy detection for spectrum sensing in cognitive radio," *IEEE Signal Process. Lett.*, vol. 15, pp. 649–652, Oct. 2008.

[36] B. Zayen, A. Hayar, and K. Kansanen, "Blind spectrum sensing for cognitive radio based on signal space dimension estimation," in *Proc. IEEE Int. Conf. Commun. (ICC)*, Jun. 2009, pp. 1–5.

[37] G. Prema and P. Gayatri, "Blind spectrum sensing method for OFDM signal detection in cognitive radio communications," in *Proc. Int. Conf. Commun. Netw. Technol. (ICCNT)*, Dec. 2014, pp. 42–47.

[38] A. Mezghani and A. L. Swindlehurst, "Blind estimation of sparse broadband massive MIMO channels with ideal and one-bit ADCs," 2017, *arXiv:1709.06698*. [Online]. Available: https://arxiv.org/abs/1709.06698

[39] G. Li, X. Zhou, Y. Jiang, L. Lin, and S. Li, "Review on automatic detection techniques of high-frequency CW signal," *World Sci-Tech R&D*, vol. 35, no. 3, pp. 337–343, 2013.

[40] P. W. Becker, *Recognition of Patterns: Using the Frequencies of Occurrence of Binary Words*. Berlin, Germany: Springer, 2013.

[41] J. Lin, G. Li, X. Zhou, D. Zhou, T. Shi, and Y. Jiang, "Study of weak high-frequency CW signal detection based on stochastic resonance," *Int. J. Model., Identificat. Control*, vol. 10, nos. 3–4, pp. 255–262, 2010.

[42] Z. Wei, K. Jia, and Z. Sun, "An automatic detection method for morse signal based on machine learning," in *Proc. Int. Conf. Intell. Inf. Hiding Multimedia Signal Process.* Cham, Switzerland: Springer, 2017, pp. 185–191.

[43] L. Cohen, "Time-frequency distributions-a review," *Proc. IEEE*, vol. 77, no. 7, pp. 941–981, Jul. 1989.

[44] S. Filin, H. Harada, H. Murakami, and K. Ishizu, "International standardization of cognitive radio systems," *IEEE Commun. Mag.*, vol. 49, no. 3, pp. 82–89, 2011.

[45] D. Freedman and P. Diaconis, "On the histogram as a density estimator: L_2 theory," *Zeitschrift für Wahrscheinlichkeitstheorie und Verwandte Gebiete*, vol. 57, no. 4, pp. 453–476, 1981.

[46] R. C. Gonzalez, *Digital Image Processing*. London, U.K.: Pearson, 2016.

[47] C. Cortes and V. Vapnik, "Support-vector networks," *Mach. Learn.*, vol. 20, no. 3, pp. 273–297, 1995.

[48] I. T. Jolliffe, "Principal component analysis for special types of data," in *Principal Component Analysis*. Berlin, Germany: Springer, 2002, pp. 338–372.

[49] W. S. McCulloch and W. Pitts, "A logical calculus of the ideas immanent in nervous activity," *Bull. Math. Biophys.*, vol. 5, no. 4, pp. 115–133, 1943.

[50] P. Vincent, H. Larochelle, I. Lajoie, Y. Bengio, and P.-A. Manzagol, "Stacked denoising autoencoders: Learning useful representations in a deep network with a local denoising criterion," *J. Mach. Learn. Res.*, vol. 11, no. 12, pp. 3371–3408, Dec. 2010.

[51] A. Paszke, S. Gross, S. Chintala, and G. Chanan. (2017). *Pytorch*. [Online]. Available: https://github.com/pytorch/pytorch

[52] M. D. Zeiler, "ADADELTA: An adaptive learning rate method," 2012, *arXiv:1212.5701*. [Online]. Available: https://arxiv.org/abs/1212.5701

YE YUAN received the B.S. degree in electronic and information engineering from the Beijing University of Technology, China, in 2013, where he is currently pursuing the Ph.D. degree with the College of Information and Communication Engineering. His current research interests include data mining, deep learning, signal processing, and bioinformatics.

ZHONGHUA SUN received the B.S. degree in electronic engineering and the M.S. and Ph.D. degree in communication and information system from Jilin University, in 2001, 2004, and 2007, respectively. Since 2007, he has been with the Faculty of the College of Electronic Information and Control Engineering, Beijing University and Technology (BJUT), where he is currently an Associate Professor with the Faculty of Information. His current research interests include video content analysis, video scene recognition, and image content annotation.

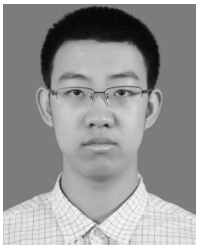

ZHIHAO WEI received the B.S. degree in electronic and information engineering from the Beijing University of Technology, China, in 2015, where he is currently pursuing the Ph.D. degree in electronic science and technology. His research interests include image processing, computer vision, and machine learning.

KEBIN JIA received the M.S. and Ph.D. degrees in information and communication engineering from the University of Science and Technology of China, in 1990 and 1998, respectively. He is currently a Professor and the Director of First-Class Disciplines Construction Office, Beijing University of Technology. He is also a Full Professor with the College of Information and Communication Engineering and the Director of the Digital Multimedia Information Processing Laboratory (MIPL). He has published more than 200 research publications and authored 2 books in these areas. He has served as PI for more than 15 research projects from The National Natural Science Foundation of China (NSFC), 973 National Basic Research Program, and 863 Program. His research interests include multimedia and database systems, content-based image/video retrieval, image/video coding and processing, data mining, and pattern recognition. He is a Senior Member of the Chinese Institute of Electronics. His group has received the award of Outstand and Innovator Group Award of the Committee of Education of Beijing.